THESIS

Under What Conditions Do Parallel Channel Networks Occur?

Submitted by

Kichul Jung

Department of Civil and Environmental Engineering

In partial fulfillment of the requirements

For the Degree of Master of Science

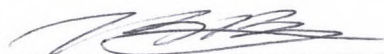Colorado State University

Fort Collins, Colorado

Fall 2010

COLORADO STATE UNIVERSITY

September 30, 2010

WE HEREBY RECOMMEND THAT THE THESIS PREPARED UNDER OUR SUPERVISION BY KICHUL JUNG ENTITLED UNDER WHAT CONDITIONS DO PARALLEL CHANNEL NETWORKS OCCUR BE ACCEPTED AS FULFILLING IN PART REQUIREMENTS FOR THE DEGREE OF MASTER OF SCIENCE.
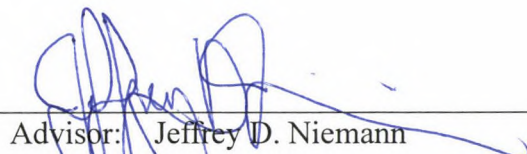
Committee on Graduate Work

_____
Xiangjiang Huang

_____
Ellen E. Wohl

_____
Advisor: Jeffrey D. Niemann

_____
Department Head: Luis A. Garcia

ii

ABSTRACT OF THESIS

UNDER WHAT CONDITIONS DO PARALLEL CHANNEL NETWORKS OCCUR?

Geologists have long recognized that channel networks can deviate from a typical

dendritic form when they develop under certain geologic or topographic constraints.

One such deviation is the so-called parallel form, which is thought to develop when the

pre-existing surface is sloping.   The objectives of this research are to determine the

specific conditions under which parallel networks occur and the nature of the transition

between dendritic and parallel networks.   Both real and simulated channel networks are

analyzed in this study.   The real networks were obtained from the digital elevation

models of basins that include large areas of the pre-existing topographic surface.   Such

areas were identified as locations with small drainage areas and topographic curvatures

that are close to zero.   For each basin, the average slope of the pre-existing surface was

calculated by averaging the local slopes for all points that are part of the pre-existing

surface.   Each channel network was then classified using a recently published method

that can distinguish five different network types (including dendritic and parallel) based

on three measures that are derived from scaling-invariance.   These measures focus on

the increments of drainage area along a channel, the irregularity of channel courses, and

the angles formed by merging tributaries. Based on these classifications, it is observed that natural networks become abruptly parallel when the average slope of the pre-existing surface exceeds about 3%. Simulated channel networks were also generated using a detachment-limited model for fluvial erosion and a slope-dependent model for hillslope processes. The parameters of the model were determined to imitate the real basins, and the average slope of the pre-existing surface was used for the slope of the initial surface. Based on these simulations, the model can also produce a transition between dendritic and parallel networks for an initial slope around 3%, but this threshold depends on the roughness of the initial surface and the boundary conditions.

Kichul Jung
Department of Civil and Environmental Engineering
Colorado State University
Fort Collins, CO 80523
Fall 2010

ACKNOWLEDGEMENTS

TABLE OF CONTENTS

LIST OF TABLES

LIST OF FIGURES

1. Introduction

Geologists have long recognized that channel networks can have significantly different features depending on the geologic and topographic constraints under which they developed. These differences have led to classifications of commonly-observed network planforms such as dendritic, parallel, and pinnate (Zernitz, 1932; Parvis, 1950; Howard, 1967), which are the focus of this paper. A dendritic network appears tree-like with wide basin shapes, relatively irregular channel courses, and tributaries that join at moderately acute angles. A parallel network has narrower basins, straighter channels, and more acute tributary junction angles. A pinnate network appears feather-like with a very straight main channel and many small tributaries joining the major channel at regular intervals and acute angles. Terms such as sub-dendritic and sub-parallel have also been used to describe networks that fall between the more basic classifications (Zernitz, 1932; Parvis, 1950; Howard, 1967). A sub-dendritic network is a network that appears mostly dendritic but tends to have its larger channels oriented in a particular direction (Parvis, 1950). A sub-parallel network is mostly parallel but lacks complete conformity to this classification. It tends to have its smaller streams oriented in a particular direction (Parvis, 1950).

Several attempts have been made to develop quantitative methods to define these classifications. Morisawa (1963) examined the orientations of first order Strahler (1952) streams for different network types. For networks that were considered dendritic, the distribution is nearly uniform. For networks that were considered parallel, she found a dominance of a single direction. Argialas et al. (1988) developed a classification system for third-order channel networks that aims to distinguish between eight different network

types including dendritic, parallel, and pinnate. This method was refined by Hadipriono et al. (1990) by implementing a knowledge-based expert system. Ichoku and Chorowicz (1994) also developed a quantitative procedure to classify networks extracted from digital elevation models (DEMs). Their method distinguishes 5 network types including dendritic, parallel, and pinnate using 16 network characteristics. None of these methods is based on a geometrical theory of network forms. Instead, they only aim to reproduce visual classifications. More recently, Mejía and Niemann (2008) developed a classification system that aims to distinguish five network types including dendritic, parallel, and pinnate by evaluating potential deviations from planform self-similarity, which is observed for dendritic networks (Veneziano and Niemann, 2000a, b). This method evaluates the accumulation of drainage area along a channel, the irregularity of channel courses, and the angles formed by merging tributaries using measures that are derived from self-similarity. Based on this approach, they confirmed that dendritic networks are self-similar, while parallel and pinnate networks are approximately self-affine (they did not consider in detail whether multi-fractality might apply). They also found that parallel and pinnate networks can be distinguished most easily by the behavior of their junction angles. For parallel networks, the average junction angle tends to increase with increasing Euclidean basin length, while for pinnate networks, the opposite behavior is observed. A classification scheme based on these measures was able to reproduce visual classifications found in the literature for 44 out of 50 test cases. It should be noted that none of these methods have quantitatively distinguished either sub-dendritic or sub-parallel networks.

Several authors have sought to determine the conditions under which dendritic,

parallel, pinnate, and related network types occur. In the early papers that present anthologies of network types, qualitative interpretations for their origins are provided (Zernitz, 1932; Parvis, 1950; Howard, 1967). A dendritic network is expected to occur when few topographic or geological constraints are present and the network freely develops. A parallel network is expected to occur when the network develops on a sloping topographic surface, although parallel topographic features or parallel faults are acknowledged as possible causes in some cases. Mosley (1972) used a 15.3 m by 9.2 m flume with artificial precipitation to study rill erosion. He observed the development of microrills that are visually consistent with a dendritic pattern on low slopes, whereas parallel patterns were produced on the steeper surfaces. In contrast, Sólyom and Tucker (2007) demonstrated using a theoretical approach that non-steady state hydrology, which is expected to occur where storms are relatively short in duration and small in size, produces optimal junction angles that increase downstream in a basin (similar to parallel networks). The origins of pinnate networks are less clear. Zernitz (1932) primarily cites topographic slope as a control, while Howard (1967) cites a combination of slope and easily erodible substrates. All of these authors faced a significant challenge in determining the physical origins of these networks because quantitative measures were not available to consistently determine network types. Phillips and Schumm (1987) hypothesized that networks progress through a continuum of network structures from dendritic, sub-dendritic, sub-parallel, parallel, and finally pinnate as the slope of the surface on which the network develops increases. To evaluate this hypothesis, they conducted eight experiments in a 2 m by 3 m flume with initial slopes ranging from 1.1% to 16.0%. To distinguish the network types, they measured the angles formed by

merging channel tributaries. The junction angle was defined using the shortest linear segment of each channel above a selected junction. They focused on so-called primary junction angles, which involve channels that form first as the channel network extends to capture the sloping terrain. Although significant scatter was observed, the average primary junction angle decreases from about 60° to approximately 43° when the initial slope increases beyond about 2% or 3%. The authors also considered a natural channel network in southern Wyoming that formed on a surface with a slope around 2.4% and has a roughly parallel form. In the end, they concluded that the networks transform from dendritic to sub-dendritic at 2% slope, to sub-parallel at 3%, and to parallel at 5% or higher. However, these transitions appear to be based on visual inspection of the networks rather than the junction angle measure, which exhibits only a single clear transition. They did not observe the occurrence of pinnate networks in their experiments.

The main objective of the present paper is to determine how natural channel networks respond to different pre-existing topographic slopes. In particular, we have three goals. First, we aim to determine whether natural networks exhibit a transition from dendritic to parallel between 2% and 3% initial slope, similar to experimental networks. Second, we aim to determine whether the transition between these two network types in nature is abrupt as suggested by Phillips and Schumm's (1987) tributary junction angle measure, or gradual as suggested by their visual interpretation of the networks. A gradual transition would provide a possible explanation for the occurrence of sub-dendritic, sub-parallel, and pinnate networks in nature. Third, we aim to determine whether factors other than slope impact the occurrence of dendritic, parallel,

14

and related drainage network types.

The general methodology is to use a mixture of data analysis and numerical modeling. In Section 2, a method is described for evaluating natural networks derived from DEMs. Regions are first identified where the channel networks have not fully extended, so portions of the pre-existing surface remain. The average slopes of these areas are then determined using a measure developed in this paper, and the network type is evaluated using the measures presented by Mejía and Niemann (2008). The results of this analysis are presented in Section 3. To assess whether other factors might affect this behavior, we also use a simple landscape evolution model to simulate the development of channel networks on surfaces with varying slopes, roughness, and boundary conditions. We then evaluate these networks using the same measures that are applied to the natural networks. The model is described in Section 4, and the simulated topographies are analyzed in Section 5. Finally, Section 6 summarizes the main conclusions of the study.

2. Methodology for Analyzing Real Basins

2.1 Evaluating Initial Topographic Slope

The first step in evaluating the dependence of network morphology on the slope of the pre-existing surface is to identify regions where the pre-existing slope can be estimated. Our strategy is to estimate this slope from portions of the region that remain relatively unaffected by the evolution of the current generation of the topography. Locations are considered to be part of the pre-existing surface if hillslope and fluvial processes have produced little alteration in the morphology of the land surface.

In order to use this approach, it is critical to select regions that have such pre-existing areas. An initial screening of regions was performed using aerial photographs and coarse elevation data. Regions were only inspected within the United States to improve the likelihood that high quality elevation data would be available for the selected sites. In the initial screening, areas were considered to have been affected by fluvial erosion if they are part of an incised valley network. Furthermore, any locations with small drainage areas were initially assumed to have been altered by hillslope processes. Thus, regions were sought with locations that have relatively large drainage areas and yet are not part of a valley network. Using this method, 30 regions were identified in Colorado, Utah, Wyoming, and Tennessee. DEMs were obtained for each region from the National Elevation Dataset. The horizontal resolution for these DEMs is 1 arc-second, which produces grid cells with a linear dimension that is approximately 30 m. For simplicity, the average grid cell dimensions are assumed to apply to all grid cells within each region (Maling, 1992; Van Sickle, 2004). Flow directions were calculated using the D8 method (O'Callaghan and Mark, 1984; Tarboton et al., 1991), which has

been shown to be adequate for analysis of channel networks (Ijjasz-Vasquez and Bras, 1995; Moglen and Bras, 1995a; Mejía and Niemann, 2008). A single large basin that includes portions of the pre-existing surface was then extracted from each region for detailed analysis. The basins identified from this procedure are listed in Table 2.1 and range in size from 25 km^2 to 757 km^2.

Next, the portions of each basin that belong to the pre-existing surface were identified. To determine whether a location has been modified by the hillslope or fluvial processes associated with currently evolving landscape, thresholds were used for the drainage area and Laplace curvature, where Laplace curvature is calculated as:

$$k = f_{xx} + f_{yy} \tag{1}$$

where f_{xx} and f_{yy} are second order derivatives in the x and y directions (Zevenbergen and Thorne, 1987; Mitášová and Hofierka, 1993). Large concave-up (negative) curvature is usually associated with points that fall within the valley network (Evans, 1972; Mitášová and Hofierka, 1993). Thus, a point is considered to be eroded by the current generation of landscape evolution processes if the curvature of the point is below a specified threshold (-0.0008 m^{-1}) or the curvature of any neighboring point is below another specified threshold (-0.001 m^{-1}). The second threshold is used to remove any point from consideration that is adjacent to a neighbor with a large negative curvature. The use of this second threshold helps exclude scattered individual points from being included as part of the pre-existing surface. In response to base level lowering, fluvial erosion is also known to produce slopes that on average have a power-law dependence on local drainage area (Willgoose et al., 1991a, b; Ijjasz-Vasquez and Bras, 1995; Moglen and Bras, 1995a, b). This behavior typically applies down to small drainage areas

where the power-law breaks down and channel heads occur (Montgomery and Dietrich, 1992; Dietrich et al., 1992, 1993; Montgomery and Foufoula-Georgiou, 1993). Although a shear-stress threshold has been shown to be more reliable than drainage area for estimating channel head locations (Montgomery and Dietrich, 1989), a point likely has been affected by fluvial erosion if its drainage area falls in the range where the power-law holds. Thus, the smallest drainage area at which this power law is observed is also used to identify fluvially-eroded points. The drainage area where the power-law begins in each basin is given in Table 2.1. A similar threshold approach is used to identify points that have been modified by hillslope processes. In response to base level lowering, hillslope processes are known to produce smooth surfaces with convex-up (positive) curvature (Evans, 1972; Mitášová and Hofierka, 1993). While this curvature is not necessarily constant at all positions on a hillslope (Roering et al., 1999), a positive curvature is expected to indicate that a point has been affected by hillslope processes. Thus, a point is considered to be eroded by hillslope processes if its curvature exceeds a specified threshold (0.0008 m^{-1}) or the curvature of any adjacent neighbor exceeds a second specified threshold (0.001 m^{-1}). Once again, the second threshold is included to ensure that pre-existing locations are located in fewer, more contiguous surfaces. If a point is not identified by any of these thresholds, it is considered to be part of the pre-existing surface. Fig. 2.1 shows examples of the pre-existing locations identified within the West Blackburn Creek basin in Tennessee (Fig. 2.1a) and the Yellow Creek Tributary 2 basin in Colorado (Fig. 2.1b). The pre-existing portions of these basins (black areas) amount to 6.10% and 2.54% of the total basin areas, respectively. Notice that the

18

remnants of the pre-existing surface are located away from the major channels due to the drainage area threshold.

It should be recognized that the identification of the pre-existing surface is necessarily speculative. It is possible that the topography of these locations has still been modified by recent fluvial, hillslope, or other processes. In particular, landsliding processes can produce surfaces with small drainage areas and constant slopes (Dietrich and Dunne, 1978; Dietrich et al., 1986; Tucker and Bras, 1998). However, such surfaces tend to have much larger slopes than those identified by this procedure (see below). It is also possible that flexural isostacy has modified the slopes of these locations in response to the unloading of the surrounding crust by the erosion processes. Thus, the present surfaces may not accurately reflect pre-existing conditions. Finally, it should also be noted that this procedure is scale dependent because the curvature is calculated over a scale that is determined by the resolution of the DEM.

The third step is to calculate the average slope for the pre-existing regions. The average slope is simply the arithmetic average of the slopes determined from each grid cell and its downstream neighbor according to the D8 algorithm. This approach is only expected to give an approximate value for the overall slope of the pre-existing surface because each local slope can be in any of the eight directions determined by the grid. However, because the pre-existing surfaces have curvatures near zero (based on the criteria used to identify them), the slope is not highly variable between locations. The histograms of the drainage directions for the pre-existing locations were examined for several of the analyzed basins. For basins that have large average slopes for the pre-existing surfaces, it was found that a large majority of the drainage directions typically

occur in one or two adjacent drainage directions. For basins with small pre-existing slopes, the drainage directions are more uniformly distributed among all eight directions. For example, 32% and 83% of the pre-existing locations have their slopes oriented in two adjacent drainage directions in West Blackburn Creek and Yellow Creek Tributary 2, which have average pre-existing slopes of 1.73% and 8.59%, respectively. Table 2.1 lists the 30 basins in order according to the average slope of their pre-existing regions. These slopes range between 1.38% and 8.67% with the steepest slopes occurring for the basins in Colorado, Utah, and Wyoming and the lowest slopes occurring in the basins in Tennessee.

2.2 Evaluating Channel Network Type

The transition between dendritic, parallel, and potentially other network types is evaluated using a framework based on scaling invariance. Mejía and Niemann (2008) developed a method to distinguish network types by comparing the network geometry to a self-affinity condition, which can be written:

$$\zeta_{\parallel}(L) =^{d} r^{-1}\zeta_{\parallel}(rL) \tag{2}$$

$$\zeta_{\perp}(L) =^{d} r^{-H}\zeta_{\perp}(rL) \tag{3}$$

In these equations, L is the Euclidean distance from the outlet of a sub-basin to its mainstream source (the mainstream is defined by following the tributary with larger drainage area at any junction). $\zeta_{\parallel}(L)$ is any linear feature that is measured parallel to the longitudinal axis of the sub-basin (this axis is defined from the mainstream source to the sub-basin outlet), and $\zeta_{\perp}(L)$ is a linear feature measured perpendicular to the

longitudinal axis. r is a selected rescaling factor, and $=^d$ indicates that the two sides of the equations have the same probability distributions. The Hurst exponent H is the self-affinity parameter, which characterizes the degree of anisotropy in the scaling condition. If $H = 1$, the equations imply self-similarity instead of self-affinity.

From this self-affinity condition, Mejía and Niemann (2008) derived three measures to characterize channel networks. The first measure focuses on the increments of drainage area along mainstreams and ultimately characterizes the horizontal shapes of sub-basins. This measure is calculated by considering a point that is some Euclidean distance L from its mainstream source. For a selected constant factor b, one can identify an upstream point that is a Euclidean distance $L - bL$ from the source. The difference in the drainage area between these two points is denoted $\Delta A_{bL}(L)$. If self-similarity holds, Mejía and Niemann (2008) showed that the probability distribution of $\Delta A_{bL}(L)/L^2$ is independent of L. Thus, a plot of $\Delta A_{bL}(L)/L^2$ against L is stationary. If self-affinity applies, then this plot will have a constant slope that is $H - 1$. The constant b determines the scale (relative to the sub-basin's size) over which the drainage area increments are calculated. As b becomes large, the range of basin sizes that can be considered decreases because the upstream point will more commonly occur in a hillslope grid cell. As b becomes small, the limitations of the grid resolution become more evident in the results of the measure. Thus, $b = 0.2$ is selected for the measure of drainage area increments based on the analysis of Mejía and Niemann (2008).

The second measure focuses on the irregularity of the channel courses. Again, it is calculated by considering a point that is Euclidean distance L from its mainstream

source and an associated upstream point that is Euclidean distance $L - bL$ from the source. Between these two points, one can calculate the standard deviation of the channel course, which is measured in the direction that is perpendicular to the longitudinal axis of the sub-basin. This standard deviation is denoted $\sigma_{bL}(L)$. If self-similarity holds, then Mejía and Niemann (2008) showed that the distribution of $\sigma_{bL}(L)/L$ is independent of L, so a plot of $\sigma_{bL}(L)/L$ against L is stationary. If self-affinity holds, then the plot has a constant slope that is $H - 1$. For this measure, $b = 0.4$ is selected based on the results of Mejía and Niemann (2008).

The third measure focuses on the angle formed by merging channels. This measure is calculated by considering any location in the channel network that is a junction of two tributaries. The orientation of the larger of the two tributaries is determined using the chord between the junction and a point that is Euclidean distance bL upstream from the junction on that tributary. Similarly, the orientation of the smaller of the two tributaries is determined using the chord between the junction and a point that is Euclidean distance bL_s upstream from the junction on the smaller tributary. The angle formed by these two chords is the junction angle and is denoted $\psi_{bL,bL_s}(L)$. If self-similarity holds, then Mejía and Niemann (2008) showed that the distribution of $\psi_{bL,bL_s}(L)$ is independent of L. Because of the way $\psi_{bL,bL_s}(L)$ is defined, a slope in the plot of $\psi_{bL,bL_s}(L)$ against L is not directly related to the Hurst exponent. $b = 0.1$ is selected for this measure in order to measure the orientations of the streams relatively close to each junction (Mejía and Niemann, 2008).

22

Using these measures, Mejía and Niemann (2008) found that parallel and pinnate networks can be distinguished from other network types because they are self-affine. In particular, if the Hurst exponent is determined from the stream course irregularity and is less than about 0.91, then the network is classified as either parallel or pinnate in their suggested algorithm. The Hurst exponent can also be estimated from the drainage area increments, but the results provide a less reliable classification (Mejía and Niemann, 2008). They also found that parallel networks can be distinguished from pinnate networks using the slope of the junction angle measure. If average slope for this measure is greater than 0.01 then the network is considered paralle. Otherwise, the network is considered pinnate (Mejía and Niemann, 2008).

Table 2.1. The 30 basins analyzed in this paper, including the outlet locations, basin sizes, the thresholds above which the approximate power-law relationship between average slope and draiange area holds, and the average slope of the pre-existing surface.

Stream Name	Latitude and Longitude of Outlet Degrees (°)	Basin Area (km^2)	Area Threshold (m^2)	Pre-existing Slope (%)
Brier Fork Creek, TN	34.928753, -86.652578	102	2×10^3	1.38
Taylor Creek, TN	35.997644, -85.613608	207	3×10^3	1.47
Little Limestone Creek, TN	34.925253, -86.807197	59	2×10^3	1.50
Walker Creek, TN	34.990444, -86.574892	61	3×10^3	1.65
West Blackburn Creek, TN	36.216181, -85.574892	62	2×10^3	1.73
Battle Creek, TN	35.064978, -85.739869	295	9×10^3	1.93
Spring Creek, TN	36.259225, -85.414064	184	4×10^3	2.00
Collins River, TN	35.566697, -85.701281	757	9×10^3	2.04
Flint Trotters Branch, TN	34.990444, -86.578408	25	3×10^3	2.08
Caney Fork Creek, TN	35.982253, - 85.159861	117	4×10^3	2.46
Sixmile Creek, UT	41.829875, - 111.141700	36	7×10^3	3.26
Scott Canyon, WY	41.680390, -109.453913	25	3×10^3	3.33
Albert Creek, WY	41.506527, -110.609580	440	1×10^4	3.79
Roubildeau Creek, CO	38.727658, -108.157822	141	5×10^3	4.02
Little Muddy Creek, WY	41.563422, -110.610314	295	1×10^4	4.13
Mancos River Trib.1, CO	37.143864, -108.429964	66	1×10^4	4.45
Mancos River Trib.2, CO	37.100375, -108.507286	109	1×10^4	4.57
Escalante Creek, CO	38.727658, -108.157822	230	2×10^4	4.84
Mancos River Trib.3, CO	37.076853, -108.554528	93	1×10^4	5.48
Trujillo Creek, CO	37.351067, -104.754483	61	6×10^3	5.62
Apishapa River, CO	37.314286, -104.755272	146	4×10^3	6.33
Black Sulphur Creek, CO	39.861680, -108.304439	235	1×10^4	6.80
Nutters Canyon, UT	40.018853, -110.318021	53	7×10^3	6.94
Duck Creek, CO	39.978750, -108.382080	114	1×10^4	7.73
Piceance Creek, CO	39.901153, -108.328089	62	1×10^4	7.98
Brundage Canyon, UT	40.025260, -110.348211	35	5×10^3	8.05
Yellow Creek Trib.1, CO	39.924997, -108.460442	84	1×10^4	8.15
Yellow Creek Trib.2, CO	39.871144, -108.487000	38	1×10^4	8.59
Greasewood Creek, CO	40.130139, -108.412640	56	1×10^4	8.62
Antelope Canyon, UT	40.035144, -110.268214	133	1×10^4	8.67

(a) West Blackburn Creek, TN   (b) Yellow Creek, Trib. 2, CO

Fig. 2.1. Illustration of the areas that are part of the pre-existing surfaces for two basins: (a) West Blackburn Creek, Tennessee, which has an average pre-existing slope of 1.73%, and (b) Yellow Creek Tributary 2, Colorado, which has an average pre-existing slope of 8.59%. Dark gray shading indicates the extent of each analyzed basin, and black shading indicates the extent of the locations that are part of the pre-existing surface within each basin.

3. Results for Real Basins

3.1 Drainage Area Increments

In this section, the measure of drainage area increments is applied to the 30 natural channel networks in order to examine the potential transition between dendritic and parallel network types. The normalized drainage area increment was calculated for all locations in each drainage network, as described in the previous section. The results were sorted according to the points' Euclidean basin lengths, and the average value of the measure was then calculated for small ranges of Euclidean basin length (Mejía and Niemann, 2008). Points with Euclidean lengths below a specified threshold for each basin are not plotted because these locations can either represent hillslopes rather than channels or their flow paths can be highly impacted by the DEM's resolution. This length threshold is selected as the smallest value that produces a channel network without a feathered appearance where straight and parallel flow paths are observed near the channel heads. This method was also used by Mejía and Niemann (2008). In Fig. 3.1a, the average drainage area increment measure is plotted as a function of Euclidean length for 6 basins, which includes 3 basins with low pre-existing slopes (1.38% − 2.46%) and 3 basins with high pre-existing slopes (4.02% − 7.73%). Fig. 3.1a suggests that the plots of the average drainage area increments tend to be approximately linear. Fluctuations are observed, particularly at large basin scales, because fewer points are available with large Euclidean lengths. Fig. 3.1a also suggests that the plots tend to be approximately horizontal (i.e., consistent with self-similarity) when the basins have low pre-existing

slopes and sloping (i.e., consistent with self-affinity) when the basins have high pre-existing slopes.

To assess the slopes observed in Fig. 3.1a, regression lines were fitted to the data and are shown by dashed lines, and the Hurst exponent H was calculated from the regression line slopes as described in the previous section. Fig. 3.1b plots the estimates of H from the drainage area increments against the pre-existing slope for each basin. The vertical line shows a Hurst exponent of 0.91, which Mejía and Niemann (2008) found could distinguish parallel and pinnate networks from other network types including dendritic, and this threshold divides the basins in Fig. 3.1b into two groups. This same division of basins can be achieved using a threshold on the pre-existing slope anywhere between 2.46% and 3.26% (the vertical dashed line shows a threshold of 2.85%, which is the midpoint of this range). In particular, when the pre-existing slope is below 3%, the average estimate of H is 1.04 with a range from 0.96 to 1.12. When the pre-existing slope is above 3%, the average estimate of H is 0.77 with a range from 0.63 to 0.90. This result suggests that the value of the pre-existing slope is related to the occurrence of dendritic and parallel networks, as suggested in the literature, and it is consistent with the experimental results of Philips and Schumm (1987), who observed a transition in network form between 2% and 3%. The value of H in Fig. 3.1b appears to be independent of the pre-existing slope below the 3% threshold. Thus, no sub-dendritic network is observed by this measure. There does seem to be either a dependence of H on the pre-existing slope among the parallel class of networks or an abrupt decrease in H that occurs when the pre-existing slope exceeds a threshold somewhere between 4.84% and 5.48% (around 5.16%, which is the midpoint of this range). From their experimental

results, Philips and Schumm (1987) suggested that a threshold occurs around 5% that distinguishes sub-parallel and parallel networks. Thus, it is possible that the networks with pre-existing slopes between about 3% and 5% are sub-parallel while the networks with slopes above about 5% are parallel. However, the values of H observed for all networks with pre-existing slopes above 3% are consistent with the results for parallel networks in Mejía and Niemann (2008), but they did not explicit consider sub-parallel networks.

3.2 Irregularity of Channel Courses

The measure of the stream course irregularity was also applied to the set of 30 basins and the results are shown in Fig. 3.2. This figure is generated using the same averaging procedure as Fig. 3.1, except that the area increment measure is replaced with the stream course irregularity measure. This plot is also expected to produce horizontal lines when self-similarity applies and negatively sloping lines when self-affinity occurs. Fig. 3.2a shows the results of the stream course irregularity measure for the same 6 basins that were plotted in Fig. 3.1a. Once again, the plots are approximately linear in all cases, and the plots are nearly horizontal when the pre-existing slope is small but have negative slopes when the pre-existing slope is large.

Fig. 3.2b plots the relationship between the estimate of H from the stream course irregularity measure and the average slope of pre-existing areas. Like the results from the measure of the drainage area increments, one observes that the basins can be efficiently divided into two groups using a threshold in H around 0.91, and one can obtain the same two groupings of basins using a threshold on the pre-existing slope

around 3%. When the pre-existing slope is below this threshold, the average estimate of H is 1.01 with a range from 0.91 to 1.07, and the value of H does not appear to depend on the value of the pre-existing slope. When the pre-existing slope exceeds 3%, the average H is 0.75, which is similar to the average estimate of H from the drainage area increments (0.77). The range of H from the stream course irregularity measure is from 0.58 to 0.87. Once again, the value of H seems to decrease as the pre-existing slope increases, which might suggest a transition from a sub-parallel to a parallel classification. However, unlike Fig. 3.1b, an abrupt change in H is not apparent around 5%. Thus, distinct sub-parallel and parallel network classifications are not apparent based on this measure.

3.3 Angles of Tributary Junctions

The measure of tributary junction angles was also applied to the 30 basin. Fig. 3.3a plots the results for the same 6 channel networks along with associated regression lines. Basins with low pre-existing slopes once again produce horizontal lines, while those with high pre-existing slopes tend to produce lines with positive slopes. The positive slopes for this measure indicate that the average tributary junction angle increases as junctions occur further downstream. The basins with high pre-existing slopes produce more variable results in Fig. 3.3a than they did when characterized with the previous two measures in Fig. 3.1a and 3.2a.

The slopes of tributary junction angle lines are plotted against the pre-existing slope for the 30 basin in Fig. 3.3b. Recall that the slope itself is not directly related to the Hurst exponent. Overall, the plot suggests that the slope of the tributary junction

angle measure is larger when the pre-existing slope is larger. Thus, the tendency of the junction angles to become larger downstream becomes more pronounced as the pre-existing slope increases. Mejía and Niemann (2008) found that the slope of the tributary junction angle measure is near zero for dendritic networks, positive for parallel networks, and negative for pinnate networks. Thus, Fig. 3.3b indicates the networks with pre-existing slopes from about 3% to almost 9% are parallel rather than pinnate. This result is interesting because several authors have suggested that large pre-existing slopes help produce pinnate networks (Zernitz, 1932; Howard, 1967; Phillips and Schumm, 1987). Fig. 3.3b also suggests that the tributary junction angle measure cannot consistently distinguish the dendritic and parallel classifications of basins. In particular, when the pre-existing slope is below 3%, the average slope of tributary junction angles is 3.03 with a range from -7.54 to 10.60. When the pre-existing slope is above 3%, the average slope of tributary junction angles is 12.98 with a range from 2.06 to 33.36. This insensitivity likely occurs because most tributaries are small relative to the mainstream at large basin sizes, and these small tributaries seem to merge with the main channel at consistent angles for both dendritic and parallel channel networks (Mejía and Niemann, 2008).

(a)

(b)
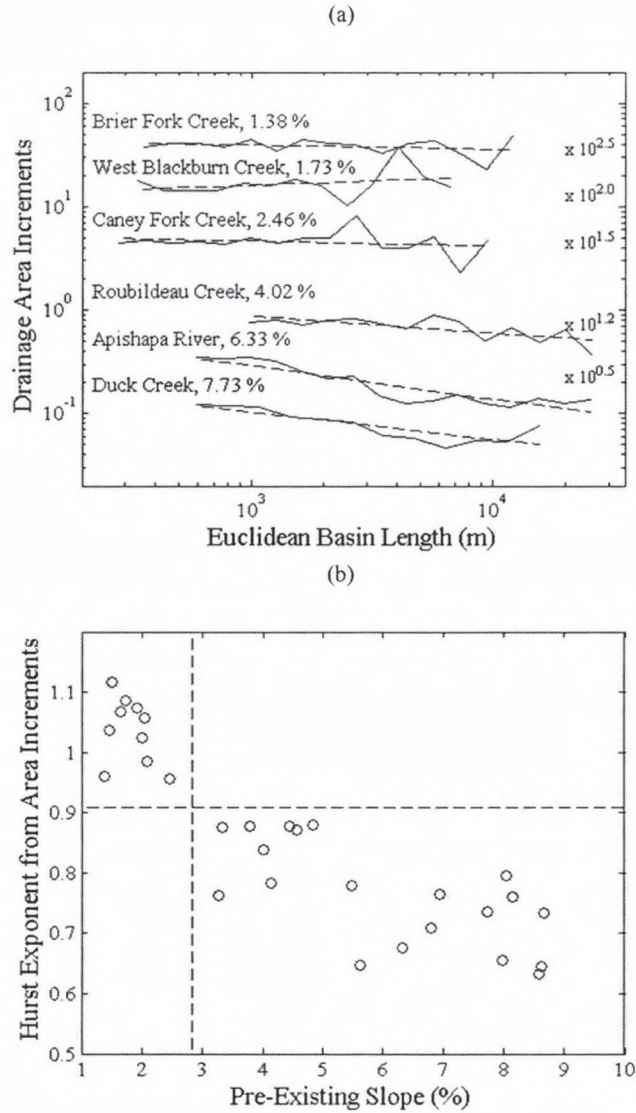
Fig. 3.1. (a) The average value of drainage area increment measure $\Delta A_{bL}(L)/L^2$ as a function of the Euclidean basin length for 6 selected basins (3 with small pre-existing slopes (1.38% – 2.46%) and 3 with large pre-existing slopes (4.02% – 7.73%)), and (b) the Hurst Exponent calculated from the drainage area increments plotted against the pre-existing slope for all 30 basins. The dashed lines in (a) are regression lines fitted to the area increment data, and in (b), they indicate thresholds that separate basins into dendritic and parallel classification based on Mejía and Niemann (2008).

31
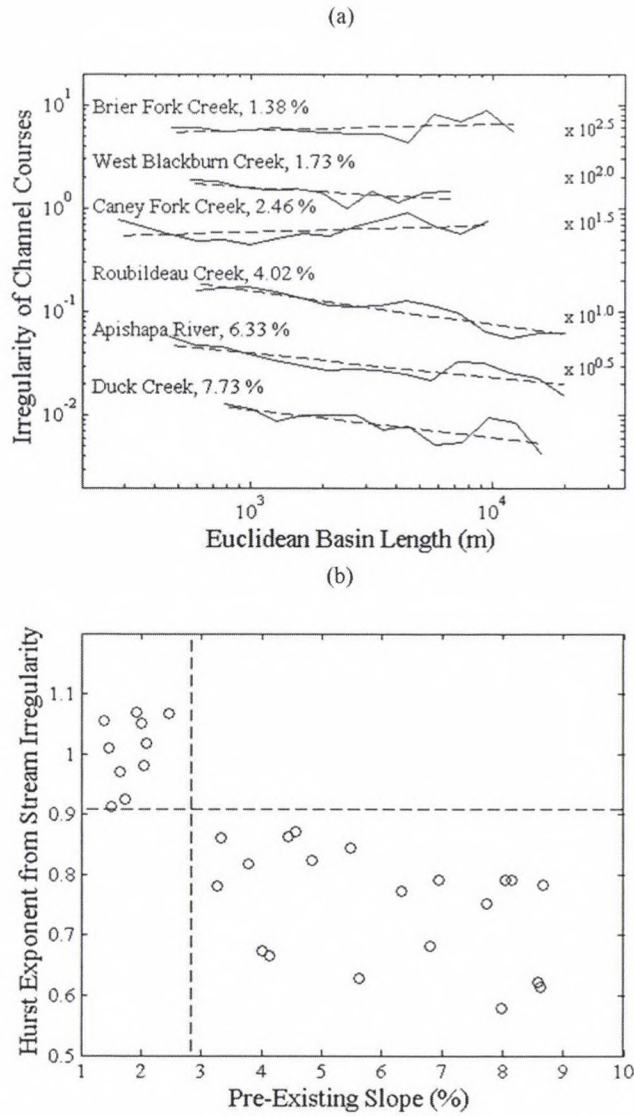
Fig. 3.2. (a) The average value of channel course irregularity measure $\sigma_{bL}(L)/L$ as a function of the Euclidean basin length for 6 selected basins (3 with small pre-existing slopes (1.38% – 2.46%) and 3 with large pre-existing slopes (4.02% – 7.73%)), and (b) the Hurst Exponent calculated from the channel course irregularity plotted against the pre-existing slope for all 30 basins. The dashed lines in (a) are regression lines fitted to the channel course irregularity data, and in (b) they indicate thresholds from Fig 3.1.
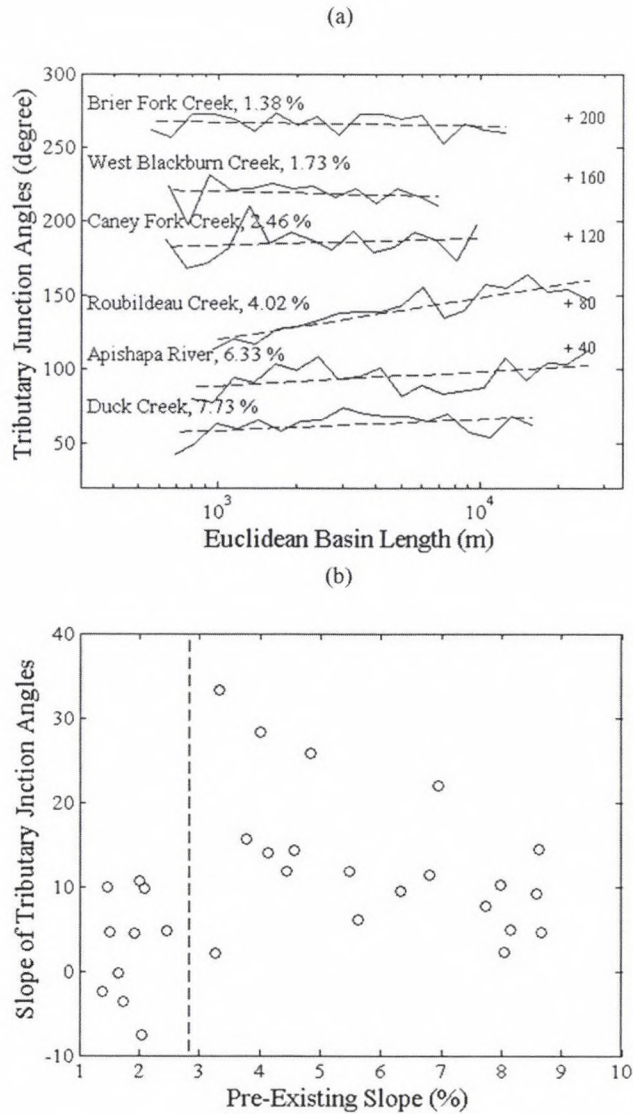
Fig. 3.3. (a) The average value of $\psi_{bL,bL_q}(L)$ as a function of the Euclidean basin length for 6 selected basins (3 with small pre-existing slopes (1.38% – 2.46%) and 3 with large pre-existing slopes (4.02% – 7.73%)), and (b) the slopes of the regression lines fitted to the data in part (a) plotted against the pre-existing slope for all 30 basins. The dashed lines in (a) are regression lines fitted to the junction angle data, and in (b) the dashed line indicates thresholds from Fig 3.1.

4. Landscape Evolution Model

We now turn to a landscape evolution model to further explore the relationship between the pre-existing slope and the channel network form. The use of a model allows us to directly specify the initial slope as well as other initial and boundary conditions. A number of quantitative models have been developed to simulate the landscape evolution (Kirkby, 1986; Ahnert, 1987; Willgoose et al., 1991a, b, c; Howard, 1994; Rigon et al., 1994; Tucker and Slingerland, 1997). These models differ in the processes that are included (fluvial, hillslope, glacial, tectonic, etc.) and in their representations of these processes. Here, we aim to use the simplest model that can produce topographies that resemble the natural basins identified earlier. Thus, the model includes only three terms: a tectonic uplift or base level lowering term, a fluvial erosion term, and a hillslope erosion term. Specifically, the evolution of local elevation z within a basin is:

$$\frac{\partial z}{\partial t} = U - \beta A^m S^n + D\nabla^2 z \qquad (4)$$

where U is a uniform uplift rate (or base level lowering rate), A is the drainage area of the point, S is the local slope, β is an erodability coefficient, m and n are erosion exponents, and D is a hillslope diffusivity. Models of this form have been used previously by Moglen and Bras (1995a, b), Niemann et al. (2003), Coleman et al. (2009) and others. The fluvial erosion term (the second term on the right-side) assumes that the detachment of material rather than the transport capacity of the flow limits fluvial erosion (Howard, 1994; Moglen and Bras, 1995a, b; Tucker and Bras, 1998). The mathematical form of this term can be derived by assuming that detachment is proportional to the shear

stress exerted by the discharge on the channel bed (Howard and Kerby, 1983; Howard, 1994; Whipple and Tucker, 1999) and by assuming that discharge is proportional to the drainage area (Kirkby, 1971; Ahnert, 1987; Tucker and Bras, 1998). This latter assumption applies when storms are long relative to the response of the basin and large relative to the size of the basin. Thus, it excludes consideration of the disequilibrium flow effects examined by Sólyom and Tucker (2007). This term also neglects any effect that sediment flux has in augmenting the detachment of material through enhanced abrasion (Whipple and Tucker, 1999). The hillslope term (the last term on the right side of the equation) can be derived by assuming that the transport of material by hillslope processes depends linearly on slope. Nonlinear models have also been suggested to describe hillslope processes (Roering et al., 1999).

The model is applied to simulate an analogue to 15 of the natural basin as follows. The simulation domain is 150 pixels by 150 pixels, and the pixel dimensions are set to match the DEM from the real basin. All boundaries are closed except for one point at the center of one edge. This point is held at a fixed elevation, and sediment and water can leave the simulation domain only at this point (the effect of the boundary conditions will be examined later). A consistent domain size and set of boundary conditions were used in all cases for simplicity because the real boundary conditions for each basin are not known. In each simulation, the initial surface is given the pre-existing slope that was determined from the DEM of the associated natural basin. In addition, random variations in elevation are superimposed on this sloping surface. These variations were drawn from a uniform distribution at every location and are uncorrelated between locations. The maximum magnitude of this noise is 7 m (the effect of this value will be

examined later). Each simulation is allowed to proceed until a steady-state condition is obtained.

The parameters of the model were estimated so that the simulated topography has a similar slope-area relationship as the observed topography. As mentioned earlier, numerous researchers have observed that a power-law relationship holds between average local slope and drainage area within the portion of the basin that is dominated by fluvial erosion. This relationship can be written:

$$S = cA^{-\theta} \tag{5}$$

where θ is typically between 0.2 and 0.6 (Hack, 1957; Flint, 1974; Tarboton et al., 1989) and c is a constant. The model also produces a power-law relationship between slope and drainage area if the topography is near steady state (so the left side of Eq. (4) is zero) and fluvial erosion is the dominant process (so the hillslope term in Eq. (4) is small). Under these assumptions, Eq. (4) can be rewritten:

$$U = \beta A^m S^n \tag{6}$$

which can be solved:

$$S = \left(\frac{U}{\beta}\right)^{\frac{1}{n}} A^{-\frac{m}{n}} \tag{7}$$

Thus, the ratio m/n can be estimated from the exponent of the observed slope-area relationship (i.e., $\theta = m/n$). Similarly, the coefficient c is controlled by the parameters U, β, and n, as shown in Eq. (7). Although D does not appear in this expression, one can show that it controls the range of drainage areas over which the power-law occurs in the model (Moglen and Bras, 1995a, b). The slope-area relationship does not contain enough information to calibrate all the model parameters,

but one can assume values for U and n without any loss of generality in the steady-state topography (Niemann et al., 2003; Coleman et al., 2009). Thus, we assume $U = 0.00001$ m/yr and $n = 1.0$. m is then estimated so that the exponent of the model's slope-area relationship matches the observed exponent, β is estimated so that the coefficient of the simulated slope-area relationship matches the observed one, and D is estimated so that the power-law relationship between slope and drainage area spans the observed range of drainage areas.

Fig. 4.1 compares the slope-area relationship for Brundage Canyon with the slope-area relationship in the associated simulated topography. The points shown in the plot represent average slopes calculated within small ranges of drainage area. The parameters of the model have been calibrated to reproduce the observed slope-area relationships, but they do not capture all the deviations from a power-law form that are observed. Although not shown in the figure due to the averaging within bins, individual slope values are much more variable in the natural basins than in the simulated basins. In addition, the simulated basins are often smaller than the observed basins due to the limited size of the computational grid. Table 4.1 summarizes the estimated parameter values for the 15 basins that were simulated with the model. This subset of basins was selected to span the observed range of pre-existing slopes as uniformly as possible.

Table 4.1. Parameters used in the landscape evolution model to generate channel networks with slope-area relationships that are similar to the analyzed natrual networks. The slope of the pre-existing surface estimated for each natural network is used as the slope for the initial topographic surface in the model simulations.

Stream Name	Initial Slope (%)	Parameters		
		$\beta(m^{1-2m}yr^{-1})$	$D(m^2/yr)$	m
Brier Fork Creek, TN	1.38	0.0000600	0.0082	0.221
Little Limestone Creek, TN	1.50	0.0000550	0.0066	0.235
Walker Creek, TN	1.65	0.0000445	0.0068	0.213
West Blackburn Creek, TN	1.73	0.0000300	0.0037	0.221
Flint Trotters Branch, TN	2.08	0.0000270	0.0048	0.247
Sixmile Creek, UT	3.26	0.00000370	0.0033	0.305
Scott Canyon, WY	3.33	0.00000300	0.0045	0.318
Mancos River Trib.2, CO	4.57	0.00000115	0.0025	0.323
Trujillo Creek, CO	5.62	0.00000105	0.0023	0.339
Apishapa River, CO	6.33	0.00000300	0.0019	0.270
Nutters Canyon, UT	6.94	0.00000220	0.0028	0.267
Duck Creek, CO	7.73	0.00000126	0.0023	0.359
Brundage Canyon, UT	8.05	0.00000480	0.0010	0.256
Yellow Creek Trib.2, CO	8.59	0.00000115	0.0030	0.326
Antelope Canyon, UT	8.67	0.00000240	0.0022	0.287
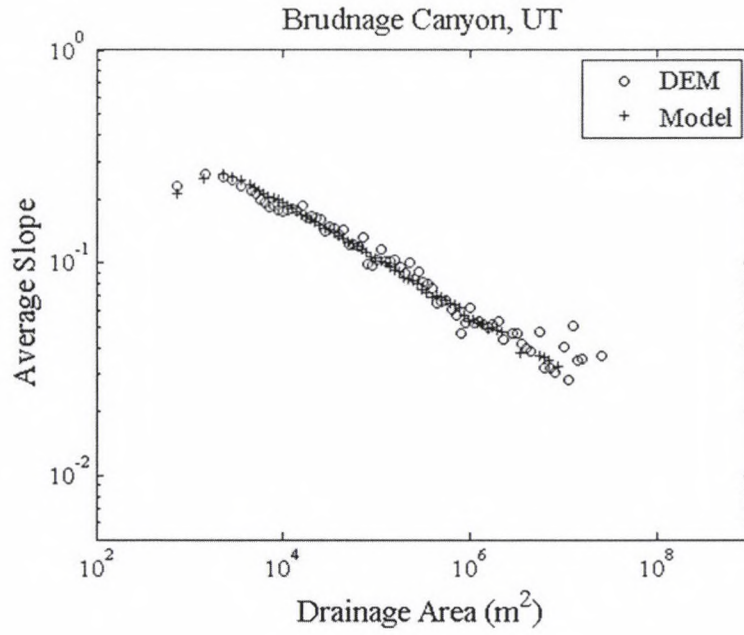
Fig. 4.1. Average local slope plotted against drainage area for Brundage Canyon, Utah (pre-existing slope: 8.05%), as determined from the DEM data and the model simulation based on the basin.

5. Results for Simulated Basins

5.1 Comparing the Simulated and Real Basins

Fig. 5.1a shows the relationship between the Hurst exponent based on the drainage area increments and the pre-existing slope for the simulated topographies, and Fig. 5.1b shows the same plot when the Hurst exponent is estimated from the stream course irregularity. In both parts of the figure, the circles show the results from the DEM analysis for comparison. Both measures suggest that the simulated basins transition between the dendritic and parallel forms (i.e. from H values above 0.91 to below 0.91) around 3%. Specifically, for the drainage area increments, the average H is 1.02 (range: 0.99 – 1.06) for the 5 simulated basins that have an initial slope less than 3%, while the average H is 0.77 (range: 0.67 – 0.84) for the 10 simulated basins that have an initial slope greater than 3%. Similarly, based on the stream course irregularity measure, the average H is 0.98 (range: 0.93 – 1.04) for simulated networks with a pre-existing slope below 3%, while the average H is 0.72 (range: 0.61 – 0.83) for the simulated networks with an initial slope above 3%. In addition, as the pre-existing slope becomes very large (particularly above about 6%), the Hurst exponent decreases further, which is similar to the behavior observed for the natural basins. The relationship between the Hurst exponent and the pre-existing slope is less erratic for the simulated basins than for the natural basins. This difference could arise from errors involved in estimating the pre-existing slope for the natural basins or from various forms of heterogeneity that are not included in the simulations but occur in reality.

The slope of the tributary junction angle measure is shown for the simulated and real basins in Fig. 5.2. When the pre-existing slope is above about 3%, the simulated

basins have positive slopes for the tributary junction angle measure. In fact, when the pre-existing slope is above 3%, the range of values for this measure does not overlap with the range for pre-existing slopes below 3%. For the 5 simulated basins with pre-existing slopes below 3%, the average slope of the tributary junction angle measure is 0.14 and the range is from -5.44 to 5.41. For the 10 simulated basins with pre-existing slopes above 3%, the average slope of tributary junction angle measure is 17.87 with the range from 11.94 to 24.06.

5.2 Effect of Surface Roughness

We now consider whether the initial surface roughness has an effect on the results by repeating all the simulations with an initial roughness magnitude of 2 m rather than 7 m. All other properties remain unchanged. Fig. 5.3a shows the relationship between the Hurst exponent (estimated from the drainage area increments) and the pre-existing slope when the roughness is 2 m and 7 m. Fig. 5.3b shows the same relationship when the Hurst exponent is estimated from the stream course irregularity. When a smaller roughness is used, the Hurst exponent decreases for simulations with low pre-existing slopes. This behavior is especially pronounced when the Hurst exponent is estimated from the stream course irregularity. If the drainage area increments are used, when the pre-existing slope is less than about 3%, the average H is 0.95 when the roughness is 2 m compared to a value of 1.02 when the roughness is 7 m. If the stream course irregularity is used instead, then the average H is 0.83 for a roughness of 2 m compared to a value of 0.98 for a roughness of 7 m. Fig. 5.4 shows the relationship between the slope of tributary junction angle measure and the pre-existing slope for the

simulated basins when different initial roughness values are used. A lower initial roughness reduces the slope of the tributary junction angle measure when the pre-existing slope is small. When the pre-existing slope is less than 3%, the average slope of tributary junction angle measure is 6.98 compared to a value of 0.14 when the roughness is 7 m. These results suggest that, in addition to the pre-existing slope, the pre-existing roughness might play a role in determining whether dendritic or parallel networks occur in nature.

5.3 Effect of Boundary Conditions

Next, we examine whether the boundary conditions affect the relationship between the pre-existing slope and the network type. In all the simulations described so far, one pixel at the midpoint of an edge of the simulation domain was held at a fixed elevation and allowed water and sediment to leave. Now, a second boundary condition is used in which an entire edge of the simulation domain is open and has a constant elevation. A third boundary condition is also used where the entire edge is open and the roughness term is also applied to the elevations of the open boundary points. All 15 basin simulations were repeated for the new boundary conditions using a roughness of 7 m.

Fig. 5.5a plots the Hurst exponent estimated from the drainage area increments for the simulations using the three boundary conditions. When an open boundary is used, the estimates of the Hurst exponent decrease, particularly for the simulations with low pre-existing slopes. If the initial slope is less than 3%, the average H is 0.83 (range: 0.78 – 0.86) when the open boundary has a constant elevation, and the average H is

0.93 (range: 0.85 – 0.99) when the open boundary has variations in elevation. For comparison, when a single point is open, the average H is 1.02 when the initial slope is less than 3%.

Similar but more pronounced results are observed when the channel course irregularity is used to estimate the Hurst exponent (Fig. 5.5b). If an open boundary is used with a constant elevation, the average H is 0.80 (range: 0.75 – 0.84) if the pre-existing slope is below 3%. If the surface roughness is applied to the open boundary, the average estimate of H is 0.80 (range: 0.74 – 0.84) when the initial slope is below the 3% threshold. For comparison, the average H is 0.98 when a single outlet is used and the initial slope is below 3%. Thus, it appears that specification of an open boundary promotes the occurrence of self-affine networks, which resemble parallel networks, even when the initial slope is low.

Fig. 5.6 shows the relationship between the slope of tributary junction angle measure and the initial slope when the different boundary conditions are used. When an open boundary is used with a constant elevation, this measure has the average slope of 10.40 (range: 2.87 – 14.91) if the initial slope is below 3%. If the boundary condition includes the surface roughness, the average slope of the measure is 6.95 (range: 3.39 – 12.07) when the initial slope is below 3%. These values are higher than those obtained for a single outlet (0.14), and they are higher than those observed for the DEMs (3.03). This measure again suggests that the use of an open boundary condition tends to produce simulated networks that resemble parallel networks even at low initial slopes.

(a)

(b)
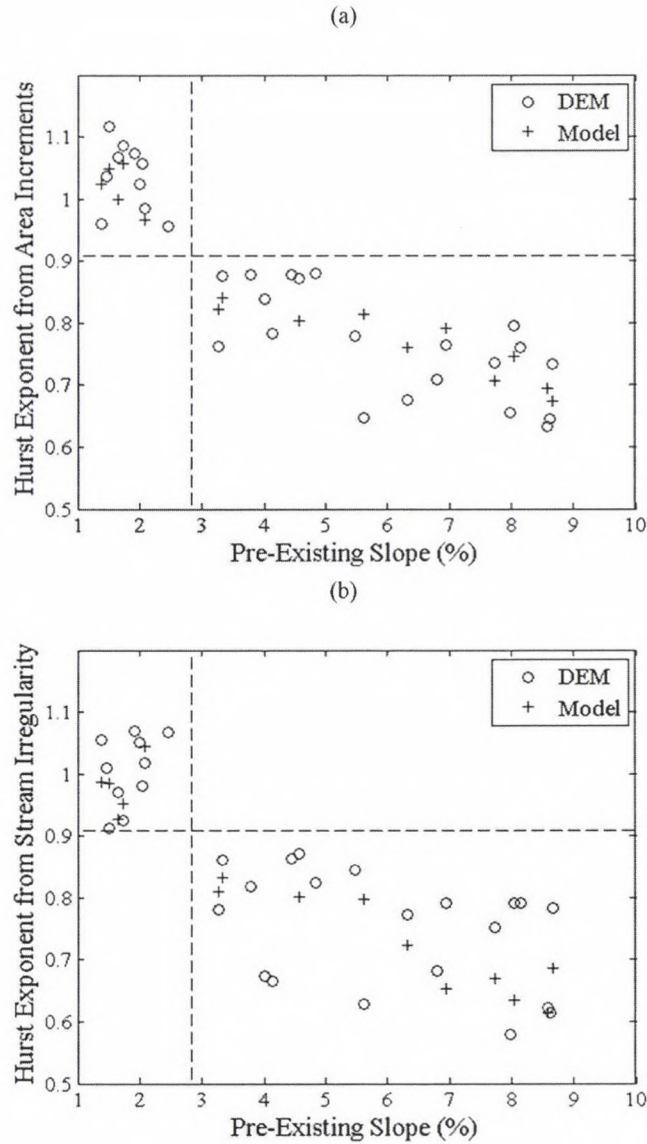
Fig. 5.1. The Hurst Exponent estimated from (a) the area increments and (b) the stream irregularity plotted against the pre-existing slope for the 30 basins delineated from DEM data and the 15 basins simulated using the model. For the modeled basins, the pre-existing slope refers to the slope of the initial topographic surface. In both parts of the figure, the dashed lines are the thresholds shown in Fig. 3.1.
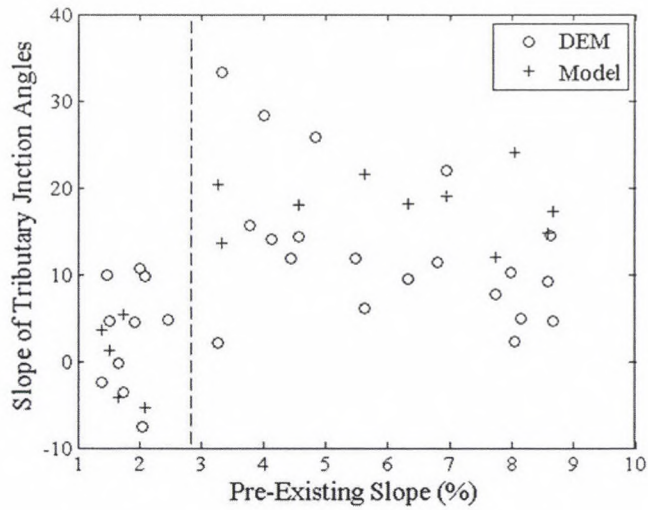
Fig. 5.2. Plot of the relationship between the slope of tributary junction angle measure and the pre-existing for the 30 basins delineated from the DEM data and the 15 basins simulated using the model. For the modeled basins, the pre-existing slope refers to the slope of the initial topographic surface. The dashed line is the threshold shown in Fig. 3.1.

(a)

(b)
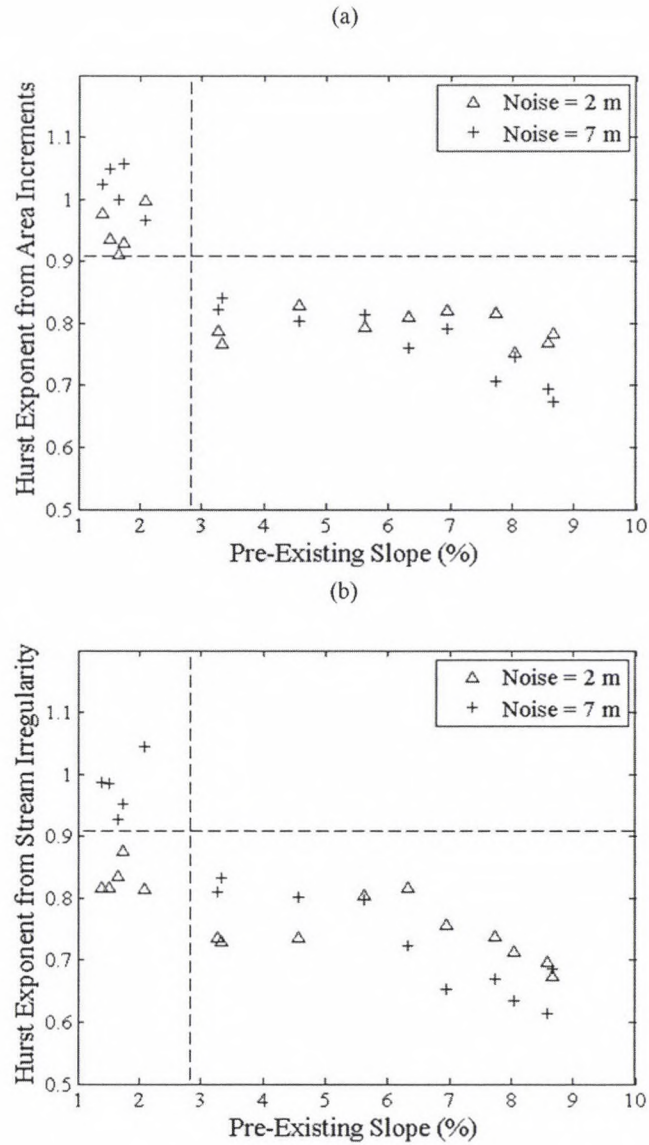

Fig. 5.3. The Hurst Exponent from (a) the area increments and (b) the stream irregularity plotted against the pre-existing slope for simulated basins when the initial roughness or noise is 2 m or 7 m as indicated in the figure. In both parts of the figure, the dashed lines are the thresholds shown in Fig. 3.1
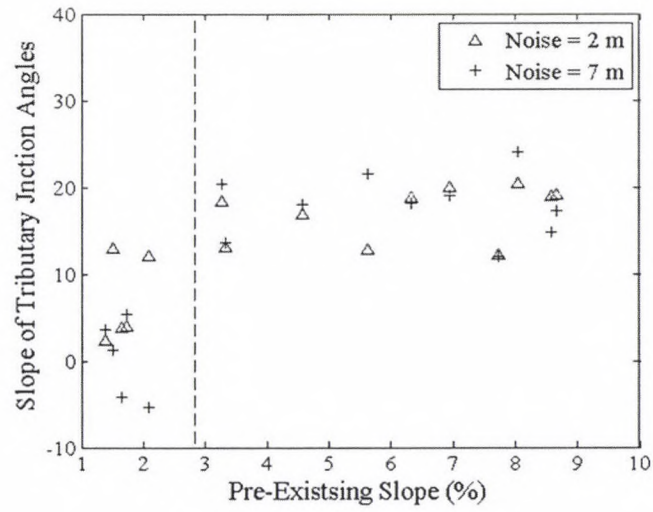
46

Fig. 5.4. Plot of the relationship between the slope of tributary junction angle measure and the pre-existing slope for simulated basins when the initial roughness or noise is 2 m or 7 m as indicated in the figure. The dashed line is the threshold shown in Fig. 3.1.
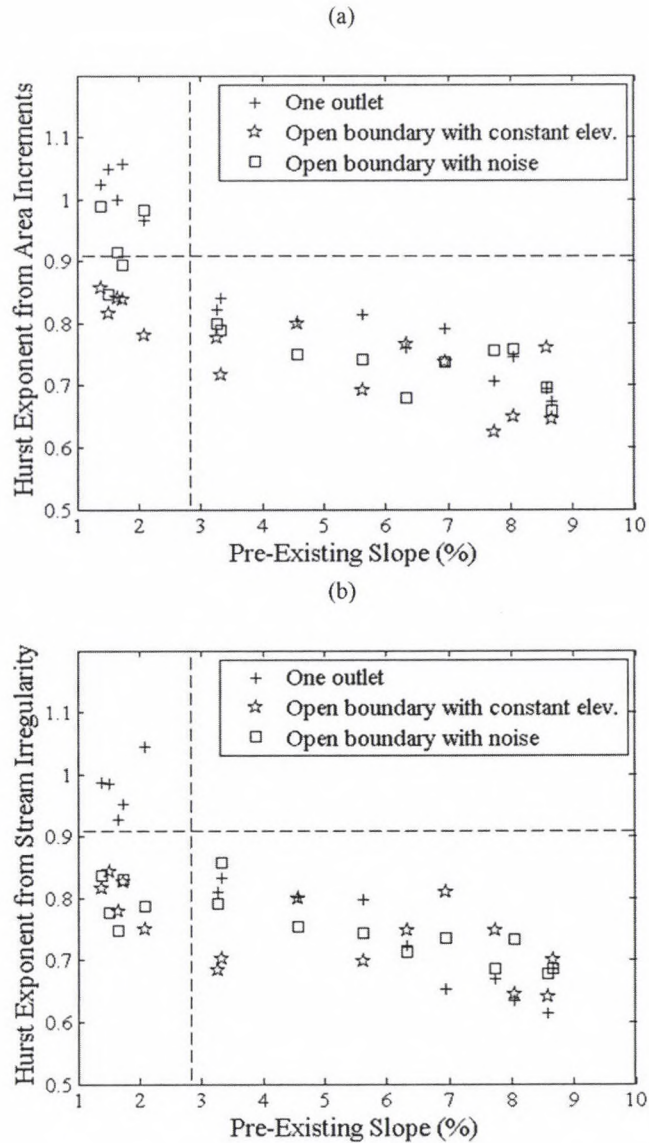
(a)

(b)

Fig. 5.5. The Hurst Exponent from (a) the area increments and (b) the stream irregularity plotted against the pre-existing slope for basins simulated using different boundary conditions as indicated in the figure. In both parts of the figure, the dashed lines are the thresholds shown in Fig. 3.1.
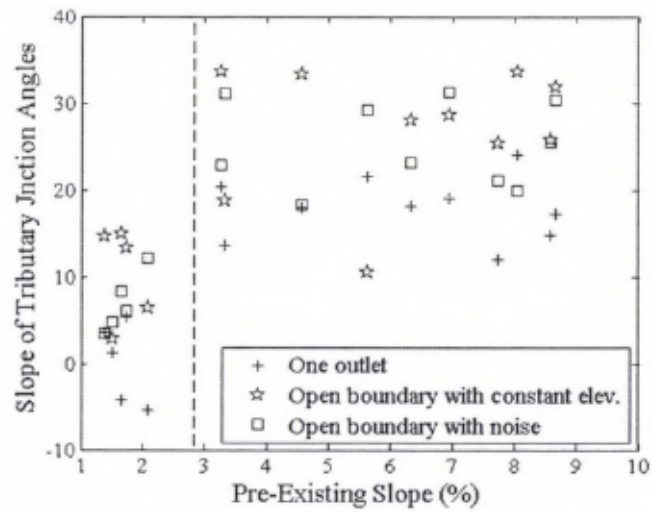
Fig. 5.6. Plot of the relationship between the slope of tributary junction angle measure and the pre-existing slope for simulated basins when different boundary conditions are used as indicated in the figure. The dashed line is the threshold shown in Fig. 3.1.

6. Conclusions

This study aimed to determine how pre-existing topographic slope affects the occurrence of dendritic, parallel, and related channel network types. Both real channel networks extracted from DEMs and simulated channel networks produced by a landscape evolution model were analyzed. In the case of the DEMs, the slope of the pre-existing surface was estimated from the average slope of areas that were identified as relatively unaffected by hillslope and fluvial processes associated with the current generation of topography. In the simulations, the pre-existing or initial slope was directly specified. The type of network was analyzed using three measures based on scaling invariance. One examined drainage area increments, another considered stream course irregularity, and the last considered tributary junction angles. Based on this analysis, the following conclusions are made:

1. The pre-existing slope is strongly related to the occurrence of dendritic or parallel networks in nature. In particular, if the pre-existing slope is below about 3%, all of the real channel networks considered in this analysis are consistent with the dendritic classification as defined quantitatively by Mejía and Niemann (2008). Specifically, they are approximately self-similar with a Hurst exponent near one, and their tributary junction angles are independent of the size of the sub-basin that is drained by the larger of the two merging tributaries. If the pre-existing slope is above about 3%, all of the real channel networks are consistent with the parallel classification as defined by Mejía and Niemann (2008). They are consistent with self-affinity, and their tributary junction angles tend to increase as the size of the sub-basin that is drained by the larger of the two merging tributaries increases.

None of the channel networks, even those with large pre-existing slopes, are consistent with the pinnate classification as defined by Mejía and Niemann (2008).

2. Within the range of pre-existing slopes that is associated with dendritic basins, all of the measures that were used to distinguish the network classifications appear to be independent of the specific value of the pre-existing slope. Thus, the measures are unable to detect the occurrence of a network form that might be called sub-dendritic. However, within the range of pre-existing slopes that is associated with the parallel classification, the measures depend on the value of the pre-existing slope. A sub-parallel classification that has entirely distinct characteristics from the parallel classification was not identified, but the network form does appear to change gradually as the pre-existing slope becomes larger.

3. The landscape evolution model can reproduce the observed transition between the dendritic and parallel network types, but the occurrence of a realistic transition depends strongly on the roughness that is added to the initial topography and the nature of the boundary conditions. In particular, specification of a smaller roughness or the use of an open boundary along an entire edge tends to promote channel networks that are more consistent with parallel networks even when the initial slope is below 3%. Because dendritic networks are consistently observed among the DEMs when the initial slope is below 3%, these dependencies are likely unrealistic and might provide avenues for further testing and improvement of landscape evolution models.

Overall, this analysis has demonstrated that the threshold between dendritic and parallel networks that was identified by Phillips and Schumm (1987) using physical

experiments also applies to real river basins. In addition, it strengthens those results by using measures of network morphology that have been shown to identify different network classifications. The presence of this threshold is important because it provides a quantitative explanation for the physical origin of parallel networks in nature, which was not considered by Mejía and Niemann (2008) in their classification method. Future research could examine whether a sub-parallel classification of networks can be defined in more detail. In addition, one could examine whether other proposed models of river basin evolution produce the observed relationship between Hurst exponent and pre-existing slope for a broader range of initial and boundary conditions.

References

Ahnert, F., 1987. Process-response models of denudation at different spatial scales. Catena, 10, 31-50.

Argialas, D., Lyon, J., Mintzer, O., 1988. Quantitative description and classification of drainage patterns. Photogrammetric Engineering and Remote Sensing, 54, 505-509.

Coleman, ML, Niemann, JD, Jacobs, EP, 2009. Reconstruction of hillslope and valley paleotopography by application of a geomorphic model. Computers & Geosciences, 35(9), 1776-1784.

Dietrich, W.E., Dunne, T., 1978. Sediment budget for a small catchment in mountainous terrain. Zietshrift fur Geomorphologie Suppl. Bd, 29, 191-206.

Dietrich, W.E., Wilson, C.J., Montgomery, D.R., McKean, J., 1993. Analysis of erosion thresholds, channel networks, and landscape morphology using a digital terrain model. The Journal of Geology, 101(2), 259-278.

Dietrich, W.E., Wilson, C.J., Montgomery, D.R., McKean, J., Bauer, R., 1992. Erosion thresholds and land surface morphology. Geology, 20(8), 675.

Dietrich, W.E., Wilson, C.J., Reneau, S.L., 1986. Hollows, colluvium, and landslides in soil-mantled landscapes. Hillslope Processes, 361-388.

Evans, I.S., 1972. General geomorphometry, derivatives of altitude, and descriptive statistics. Durham Univ (England) Dept of Geography.

Flint, J.J., 1974. Stream gradient as a function of order, magnitude, and discharge. Water Resources Research, 10(5), 969-973.

Hack, J.T., 1957. Studies of longitudinal stream profiles in Virginia and Maryland. United

States Geological Survey Professional Paper, 292, 45-97.

Hadipriono, F.C., Lyon, J.G., Li, W.H., 1990. The development of a knowledge-based expert system for analysis of drainage patterns. Photogrammetric Engineering and Remote Sensing (USA).

Howard, A.D., 1967. Drainage analysis in geologic interpretation: a summation. American Association of Petroleum Geologists Bulletin, 51(11), 2246-2259.

Howard, A.D., 1994. A detachment-limited model of drainage basin evolution. Water Resources Research, 30(7), 2261-2286.

Howard, A.D., Kerby, G, 1983. Channel changes in badlands. Geological Society of America Bulletin, 94(6), 739.

Ichoku, C., Chorowicz, J., 1994. A numerical approach to the analysis and classification of channel network patterns. Water Resources Research, 30(2), 161-174.

Ijjasz-Vasquez, E.J., Bras, R.L., 1995. Scaling regimes of local slope versus contributing area in digital elevation models. Geomorphology, 12(4), 299-311.

Kirkby, M.J., 1971. Hillslope process-response models based on the continuity equation. Institute of British Geographers Special Publication, 3, 15-30.

Kirkby, M.J., 1986. A two-dimensional simulation model for slope and stream evolution. Hillslope Processes, 203-222.

Maling, D.H., 1992. Coordinate systems and map projections. Oxford.

Mejía, A.I., Niemann, J.D., 2008. Identification and characterization of dendritic, parallel, pinnate, rectangular, and trellis networks based on deviations from planform self-similarity. Journal of Geophysical Research, 113(F2), F02015.

Mitášová, H., Hofierka, J., 1993. Interpolation by regularized spline with tension: II.

Application to terrain modeling and surface geometry analysis. Mathematical Geology, 25(6), 657-669.

Moglen, G.E., Bras, R.L., 1995a. The effect of spatial heterogeneities on geomorphic expression in a model of basin evolution. Water Resources Research, 31(10), 2613-2623.

Moglen, G.E., Bras, R.L., 1995b. The importance of spatially heterogeneous erosivity and the cumulative area distribution within a basin evolution model. Geomorphology, 12(3), 173-185.

Montgomery, D.R., Dietrich, W.E., 1989. Source areas, drainage density, and channel initiation. Water Resources Research, 25(8), 1907-1918.

Montgomery, D.R., Dietrich, W.E., 1992. Channel initiation and the problem of landscape scale. Science(Washington), 255(5046), 826-826.

Montgomery, D.R., Foufoula-Georgiou, E., 1993. Channel network source representation using digital elevation models. Water Resources Research, 29(12), 3925-3934.

Morisawa, M., 1963. Distribution of stream-flow direction in drainage patterns. The Journal of Geology, 71(4), 528-529.

Mosley, M.P., 1972. An experimental study of rill erosion. Fort Collins, Colorado State University, 99.

Niemann, J.D., Bras, R.L., Veneziano, D., 2003. A physically based interpolation method for fluvially eroded topography. Water Resources Research, 39(1), 1017.

O'Callaghan, J.F., Mark, D.M., 1984. The extraction of drainage networks from digital elevation data. Computer vision, graphics, and image processing, 28(3), 323-344.

Parvis, M., 1950. Drainage pattern significance in airphoto identification of soils and

bedrocks. Highway Research Board.

Phillips, L.F., Schumm, S.A., 1987. Effect of regional slope on drainage networks. Geology, 15(9), 813.

Rigon, R., Rinaldo, A., Rodriguez-Iturbe, I., 1994. On landscape self-organization. Journal of Geophysical Research, 99(B6), 11971.

Roering, J.J., Kirchner, J.W., Dietrich, W.E., 1999. Evidence for nonlinear, diffusive sediment transport on hillslopes and implications for landscape morphology. Water Resources Research, 35(3), 853-870.

Sólyom, P.B., Tucker, G.E., 2007. The importance of the catchment area-length relationship in governing non-steady state hydrology, optimal junction angles and drainage network pattern. Geomorphology, 88(1-2), 84-108.

Strahler, A.N., 1952. Hypsometric (area-altitude) analysis of erosional topography. Geological Society of America Bulletin, 63(11), 1117.

Tarboton, D.G., Bras, R.L., Rodriguez-Iturbe, I., 1989. Scaling and elevation in river networks. Water Resources Research, 25(9), 2037-2052.

Tarboton, D.G., Bras, R.L., Rodriguez-Iturbe, I., 1991. On the extraction of channel networks from digital elevation data. Hydrological Processes, 5(1), 81-100.

Tucker, G.E., Bras, R.L., 1998. Hillslope processes, drainage density, and landscape morphology. Water Resources Research, 34(10), 2751-2764.

Tucker, G.E., Slingerland, R., 1997. Drainage basin responses to climate change. Water Resources Research, 33(8), 2031-2047.

Van Sickle, J., 2004. Basic GIS coordinates. CRC.

Veneziano, D., Niemann, J.D., 2000a. Self-similarity and multifractality of fluvial erosion

topography 1. Mathematical conditions and physical origin. Water Resources Research, 36(7), 1923-1936.

Veneziano, D., Niemann, J.D., 2000b. Self-similarity and multifractality of fluvial erosion topography 2. Scaling properties. Water Resources Research, 36(7), 1937-1951.

Whipple, K.X., Tucker, G.E., 1999. Dynamics of the stream-power river incision model: Implications for height limits of mountain ranges, landscape response timescales, and research needs. Journal of Geophysical Research, 104(B8), 17661.

Willgoose, G., Bras, R.L., Rodriguez-Iturbe, I., 1991a. A coupled channel network growth and hillslope evolution model 1. Theory. Water Resources Research, 27(7), 1671-1684.

Willgoose, G., Bras, R. L., Rodrigueziturbe, I., 1991b. A coupled channel network growth and hillslope evolution model 2. Nondimensionalization and applications. Water Resources Research, 27(7), 1685-1696.

Willgoose, G.R., Bras, R.L., Rodriguez-Iturbe, I., 1991c. A physically based coupled network growth and hillslope evolution model: 1 Theory. Water Resources Research, 27(7), 1671-1684.

Zernitz, E.R., 1932. Drainage patterns and their significance. The Journal of Geology, 40(6), 498-521.

Zevenbergen, L.W., Thorne, C.R., 1987. Quantitative analysis of land surface topography. Earth Surface Processes and Landforms, 12(1), 47-56.